ISSN 1063-7729, Astronomy Reports, 2010, Vol. 54, No. 10, pp. 932–939. © Pleiades Publishing, Ltd., 2010.
Original Russian Text © S.V. Kalenskii, S. Kurtz, V.I. Slysh, P. Hofner, C.M. Walmsley, L.E.B. Johansson, P. Bergman, 2010, published in Astronomicheskiĭ Zhurnal, 2010, Vol. 87, No. 10, pp. 1012–1020.

VLA Observations of Class I Methanol Masers in the Region of Low-Mass Star Formation L1157

S. V. Kalenskii[1*], S. Kurtz[2], V. I. Slysh[†1], P. Hofner[3,4,5], C. M. Walmsley[6], L. E. B. Johansson[†7], and P. Bergman[7]

[1] *Astro Space Center, Lebedev Physical Institute, Moscow, Russia*
[2] *Centro de Radioastronomia y Astrofizika, Universidad Nacional Autonoma de Mexico, Mexico*
[3] *Physics Department, New Mexico Institute of Technology, Socorro, NM, USA*
[4] *National Radio Astronomy Observatory, Socorro, NM, USA*
[5] *Max-Planck-Institut für Radioastronomie, Bonn, Germany*
[6] *Osservatorio Astrofisico di Arcetri, Florence, Italy*
[7] *Onsala Space Observatory, Onsala, Sweden*

Received March 1, 2010; in final form, April 2, 2010

Abstract—We present the results of VLA observations of a maser candidate in the low-mass star formation region L1157 in the $7_0-6_1A^+$ transition at 44 GHz. The line is emitted by a compact, undoubtedly maser source associated with clump B0a, which is seen in maps of L1157 in thermal lines of methanol and other molecules. A much weaker compact source is associated with clump B1a, which is brighter than B0a in thermal methanol lines. The newly detected masers may form in thin layers of turbulent post-shock gas. In this case, the maser emission may be beamed, so that only an observer located in or near the planes of the layers can observe strong masers. On the other hand, the maser lines are double with a "red" asymmetry, indicating that the masers may form in collapsing clumps. A detailed analysis of collapsing-cloud maser models and their applicability to the masers in L1157 will be developed in subsequent papers.

DOI: 10.1134/S1063772910100069

1. INTRODUCTION

Bright and narrow maser lines of methanol (CH_3OH) have been found towards many star-forming regions [1–3]. According to the classification of Menten [4], methanol masers can be divided into two classes, I and II, with each class characterized by a certain set of transitions. The Class I maser transitions are the $7_0-6_1A^+$ transition at 44 GHz, $4_{-1}-3_0E$ transition at 36 GHz, $5_{-1}-4_0E$ transition at 84 GHz, $8_0-7_1A^+$ transition at 95 GHz, etc., while the Class II transitions are the $5_1-6_0A^+$ transition at 6.7 GHz, $2_0-3_{-1}E$ transition at 12 GHz, the $J_0-J_{-1}E$ series of transitions at 157 GHz, etc. A list of the most powerful Class I and II transitions is presented in, e.g., [5]. Both Class I and Class II masers are often overlaid on broad thermal lines. According to current views on methanol excitation, Class I masers are collisionally pumped, while Class II masers are pumped by external IR radiation [6].

The nature of methanol masers is still unknown. Plambeck and Menten [7] suggested that Class I masers arise in post-shock gas in the wings of bipolar outflows, where the abundance of methanol is enhanced due to grain-mantle evaporation. This hypothesis has further support in the fact that Class I masers in a number of star-forming regions appear to be associated with outflows [3, 8]. However, this view is not generally accepted, because there are no high-velocity Class I masers, and the apparent association between the masers and outflows may come about because both of them arise in the same star-forming regions, rather than through a physical association between these objects.

Difficulties in studies of methanol masers arise partly because, until recently, they have been observed only in regions of massive star formation, which are relatively distant (2–3 kpc from the Sun or farther) and highly obscured at optical and even NIR wavelengths. In addition, high-mass stars usually form in clusters. These properties make it difficult to resolve maser spots and to associate masers with other objects in these regions. In contrast, regions of

[†] Deceased.
[*] E-mail: kalensky@asc.rssi.ru

Table 1. Main parameters of the observed lines and of the VLA at the line frequencies

Transition	Frequency (GHz)	$S\mu^2$ (Debye)[a]	HPBW (″)[b]	G(mJy per beam)/K
$7_0 - 6_1A^+$	44.069476	6.1380	$1.87'' \times 1.45''$	7
$1_0 - 0_0A^+$	48.372467	0.8086	–	7
$1_0 - 0_0E$	48.376889	0.8084	–	7

[a] The product of the permanent dipole moment and the line strength from [11].
[b] Half-power beamwidth of the CLEAN beam.

low-mass star formation are much more widespread, and many are only 200–300 pc from the Sun; they are less heavily obscured than regions of high-mass star formation, and there are many isolated low-mass protostars. Therefore, studies of masers in these regions might be more straightforward than in the case of high-mass regions, and the detection of Class I masers in low-mass regions could have a strong impact on our understanding of masers.

Bearing this in mind, we performed in 2004 a "snapshot" search for Class I methanol masers towards bipolar outflows driven by Class 0 and I low-mass Young Stellar Objects (YSOs) at 44, 84, and 95 GHz, continuing this search in 2007 and 2008 at 44 and 36 GHz [9, 10]. The search was successful: four maser candidates in star-forming regions NGC 1333I4A, NGC 1333I2A, HH25, and L1157 were found at 44 GHz. Towards two of these, NGC 1333I4A and HH 25MMS, maser candidates were also detected at 95 GHz. One more maser candidate was detected in NGC 2023 at 36 GHz. Thus, the search results suggest that Class I masers can exist in regions of low-mass star formation, and that they can be related to bipolar outflows. However, only interferometric observations can establish whether the detected maser candidates are indeed sufficiently bright and compact to be masers. Therefore, we observed the newly detected maser candidate in L1157 at 44 GHz with the NRAO Very Large Array (VLA)[1] .

The L1157 dark cloud in Cepheus harbors a Class 0 protostar (IRAS 20386+6751), which powers a well-collimated bipolar outflow. Distance estimates vary between 200 and 450 pc [12]. The maser candidate in the L1157 outflow was selected for interferometric observations because this outflow is isolated, without known confusion of flows from other sources in the surrounding region. Bachiller et al. [13] found that the abundance of methanol is strongly enhanced towards the blue wing of the outflow. Gueth et al. [14, 15] obtained interferometric CO and SiO observations of the blue wing and found two limb-brightened cavities. To explain this, they suggested that the cavities were excavated by two flare episodes in a precessing outflow. Bachiller et al. [16] mapped L1157 in lines of methanol and other molecules with the 30-m Pico Veleta radio telescope. They found an extended region of methanol emission, with the brightest clumps, called B0, B1, and B2, related to outflow wings. The interferometric observations of Benedettini et al. [17] in 2_K-1_K thermal methanol lines resolved B0, B1, and B2 into a number of smaller clumps, which are mostly located near the edges of the cavities detected by Gueth et al. [14, 15].

In addition to 44 GHz, we observed L1157 in the thermal 1_0-0_0 A^+ and E methanol lines at 48 GHz (Table 1). The motivation for the 48-GHz observations is as follows. It is not known exactly what the maser spots are: for example, they may represent favorable lines of sight with long coherent gain paths in turbulent clouds, or discrete objects. Liechti and Walmsley [18] used the Plateau de Bure interferometer to search for thermal emission of the 2_K-1_K transitions (96 GHz) in the DR21 complex. They concluded that, if there is any thermal emission from the maser spots, it is strongly diluted by their 3.5″ beam, and suggested that the size of the masing zone is about 0.5″ or 1000 AU for DR21OH and DR21W. We decided to test this model with higher spatial resolution, realized both by the higher angular resolution of the VLA and the smaller distance of our target source.

2. OBSERVATIONS AND DATA REDUCTION

The observations were obtained on March 17, 2007 with the VLA in the D configuration, which provides an angular resolution about 1″ at 44 GHz. The observations were made with a 3.125-MHz bandwidth in right-circular polarization. For the 44 GHz line, the correlator setup provided a velocity resolution of 0.17 km/s and velocity coverage of 21.3 km/s.

To cover the entire blue wing of the outflow, we observed two positions with the J2000.0 equatorial

[1] The National Radio Astronomy Observatory is operated by Associated Universities, Inc., under contract with the National Science Foundation

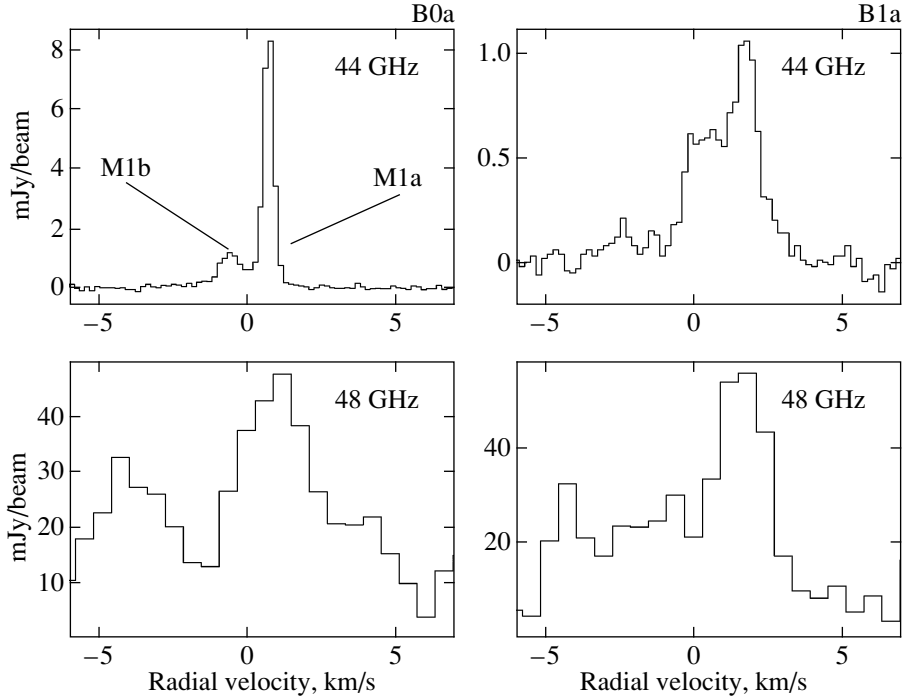

Fig. 1. VLA spectra obtained towards M1 (left panels) and M2 (right panels)at 44 GHz (upper panel) and 48 GHz (lower panel).

coordinates RA = $20^h39^m09^s.00$, Dec = $68°01'42''.0$ and RA = $20^h39^m13^s.00$, Dec = $68°00'55''$ (J2000.0). The observations were made in a fast-switching mode using the quasar 1331+305 (3C286) as a primary calibrator and 19278+73580 as a secondary calibrator. The data were reduced using the NRAO Astronomical Image Processing System (AIPS) package. After the standard calibration procedure, images were created with the task IMAGR applying CLEANing. The positions of individual features were determined using the task JMFIT.

The $1-0$ lines of A^+ and E methanol at 48 GHz were observed simultaneously using IF mode 2, each with a 6.25 MHz bandwidth and 97.656 kHz spectral resolution. The data were reduced in the same way as those at 44 GHz.

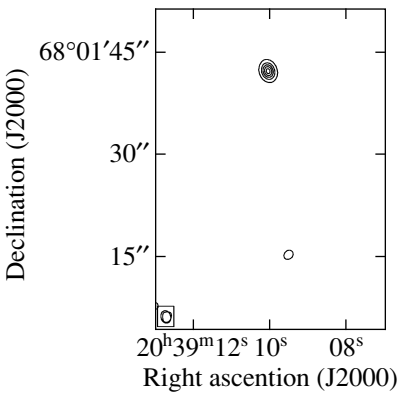

Fig. 2. Map of the blue wing of the L1157 bipolar outflow at 44 GHz obtained with the VLA. The circle in the left lower corner shows the CLEAN beam. The peak value of outflow is 1.4293 Jy/beam; isolevels corresponds to 1, 3, 5, 7, 9 in units of 0.1429 Jy/beam.

3. RESULTS

Results of the observations are presented in Table 2 and Fig. 1, 2. We detected a double source near the peak of clump B0a.[2] The two components, which we call M1a and M1b, have a formal RA offset between their peaks of $\approx 0.5''$, which is less than half the synthesized beam. Therefore, it is not clear whether these are two different components or a single region whose brightness varies with radial velocity. The source spectrum in the 1a direction is shown in Fig. 1 (upper left panel). The line consists of two components: a stronger one at 0.8 km/s, and a weaker one, probably related to 1b, at −0.5 km/s. The peak flux density of the stronger component corresponds to a brightness temperature higher than 2000 K, showing that this component is undoubtedly a maser. Since

[2] The notation for clumps in the blue wing of the L1157 outflow is taken from [17].

the source was unresolved in the D configuration, higher resolution observations are desirable.

A much weaker source, called M2, was detected near the edge of clump B1a. Its spectrum is shown in Fig. 1 (upper right panel). The brightness temperature of M2, about 200 K, is higher than the gas kinetic temperature in the B1 region (about 80 K), suggesting that this source is a weak maser. Although the nature of M2 is unclear, for simplicity, we will refer to it as a maser.

Finally, we detected weak emission in the $1_0-0_0A^+$ line at 48 GHz towards M2, and tentatively detected even weaker emission towards M1 (see Fig. 1, lower panel). However, the lines were too weak to obtain a reliable map, or even to determine source sizes. No emission was observed at the frequency of the 1_0-0_0E line.

4. DISCUSSION

Figure 2 shows the map of the blue wing of L1157 at 44 GHz obtained with the VLA. Comparison of this map with the maps of this source in HCN and CH_3OH from [17] shows that the stronger maser (M1) is associated with the clump B0a and located near the edge of the cavity excavated during the later burst of outflow activity. The weaker maser (M2) is associated with the clump B1a and is located near the terminal point of the same cavity.

A simple and natural mechanism for methanol maser emission was considered by Sobolev et al. [19]. This mechanism is based on the fact that Class I transitions are usually inverted in Galactic molecular clouds [20, 21]. Sobolev et al. [19] suggested that compact maser spots arise in extended, turbulent clouds due to the fact that, in a turbulent velocity field, the coherence lengths along some directions are longer than the mean coherence length, resulting in a random increase in the magnitude of the optical depth along certain lines in a cloud. The maser intensity of unsaturated masers is proportional to $\exp(|\tau|)$, leading to the appearance of bright spots toward lines with higher optical-depth magnitudes. Sobolev et al. [19] studied Class I J_2-J_1E masers, but most of their results are applicable to any inverted line. Thus, we can use the results of Sobolev et al. [19] to try to understand whether the masers in L1157 can be explained by the effects of turbulence.

One of the main parameters applied in [19] is τ_0—the optical depth through the source at the center of the spectral line when there is no turbulence. An upper limit for this quantity can be estimated from the equation

$$\tau_0 \leq \frac{c^2 A_{ul}}{8\pi\nu^2\delta\nu} N_u, \qquad (1)$$

where c is the speed of light, ν and A_{ul} are the line frequency and Einstein A coefficient, N_u is the column density of methanol at the upper energy level, and $\delta\nu \approx 1.06\Delta\nu$, where $\Delta\nu$ is the FWHM of the line profile when there is no turbulence. N_u can be estimated from the relation

$$\frac{N_u}{g_u} = \frac{N}{Q_{\rm rot}} \exp\left(\frac{-E_u}{kT_{\rm rot}}\right), \qquad (2)$$

where N is the methanol column density, $Q_{\rm rot}$ the rotational partition function, and E_u the upper level energy; we consider the rotational temperature $T_{\rm rot}$ to be equal to the kinetic temperature $T_{\rm kin}$. Estimates of the kinetic temperature of B0a vary approximately between 40 K and 80 K [16, 17]. Adoptng for B0a $T_{\rm kin} = 80$ K and $N \approx 10^{16}$ cm^{-2} [17], we obtain $\tau_0 \leq 10$. An optical depth of order 10 can provide maser amplification of order 20 000, which, in turn, can explain the observed maser brightness. However, we find that a single peak dominates the emission of B0a at 44 GHz, whereas Sobolev et al. [19] argued that, in general, a single peak dominates when τ_0 is of the order of at least 20–30, appreciably higher than our derived upper limit for B0a. Thus, a comparison of our results with those of Sobolev et al. [19] suggest that it is unlikely that M1 arises in a uniform clump purely as a result of turbulence (though this is not impossible, since turbulence is a stochastic process). An additional argument against this picture is that there are no masers in clumps with higher methanol column densities, and hence higher τ_0 values, than that of B0a (see Fig. 2).

Our results for M1a,b can be explained using the shock model proposed by Plambeck and Menten [7]. Observations of shock tracers such as SiO and H_2 [15, 22] show that there are shocks toward or near the maser. The shock can naturally explain the enhanced CH_3OH abundance, as a result of grain-mantle evaporation. Figure 1 from [17] suggests that the shock propagates nearly perpendicular to the line of sight near M1a,b, so that the line-of-sight velocity of the post-shock gas coincides with that of the ambient material. Moreover, the post-shock gas may be flattened in the direction of propagation of the shock. As a result, the methanol column density and optical depths of methanol lines would be lower in this direction than in any perpendicular direction. If the masers are unsaturated, the intensity of the maser emission is proportional to $\exp(|\tau|)$. Therefore, in the shock model, the maser emission is probably beamed, with the strongest masers arising perpendicular to the direction of shock propagation. This model can probably explain why the strongest maser is related to clump B0a rather than to clumps in the B1 region, where the thermal methanol emission is stronger than

Table 2. Parameters of maser sources from the VLA observations. Maximum (superscript) and minimum (subscript) values are indicated for the major and minor axes and the position angle. The RA error is in seconds of time, and the DEC error in arcsec

Source	RA (J2000) (h m s)	DEC (J2000) (° ′ ″)	Major axis (″)	Minor axis (″)	Pos. angle (°)	V_{LSR}, (km/s)
M1a	20 39 10.033 (0.001)	68 01 42.20 (0.007)	$0.4^{0.5}_{0.3}$	$0.2^{0.3}_{0.0}$	8^{163}_{51}	0.8
M1b	20 39 10.107 (0.009)	68 01 42.42 (0.063)	$0.6^{1.1}_{0.0}$	$0.4^{1.0}_{0.0}$	165^{30}_{125}	−0.5
M2	20 39 09.465 (0.035)	68 01 15.59 (0.204)	$1.9^{2.6}_{0.9}$	$0.7^{1.7}_{0.0}$	129^{165}_{90}	1.7

in B0. One possibility is that the beaming of the masers in the latter clumps is not towards us.

A more realistic model involves both these mechanisms of maser formation, i.e., the maser clumps form in edge-on, turbulent, post-shock layers. The fairly high methanol column density in such layers provides high τ_0 values, which, in turn, make it possible to explain the high-brightness maser lines and dominance of single spots using the results of Sobolev et al. [19].

Note that the B0, B1, and B2 clumps are usually considered to consist of shock-processed gas, but our model requires additional shock structures with angular sizes much smaller and methanol column densities higher than those of B0a or B1a. Therefore, a crucial test for this model is provided by observations of shock tracers such as SiO with spatial resolution higher than that of Benedettini et al. [17], in order to search for such structures.

Another model for Class I maser formation was studied by Liechti and Walmsley [18], who analysed the $8_0-7_1A^+$ Class I maser transition at 95 GHz in the high-mass star-forming region DR21(OH). They suggested that masers can arise in compact clumps with the same sizes as the individual masers. Substituting the parameters of the $7_0-6_1A^+$ transition into their Eqs. (1) and (2), we obtain for the methanol column density

$$N_{CH_3OH} = 1.6\times10^{12}T_{rot}^{1.5}e^{65/T_{rot}}\frac{\tau\Delta v}{1-e^{-2.11/T_{ex}}} \quad (3)$$

Here, T_{rot} is the rotational temperature of methanol, which is of the order of the gas kinetic temperature. T_{ex}, τ, and Δv are the excitation temperature, optical depth, and width of the $7_0-6_1A^+$ line. Equation (3) shows that N_{CH_3OH} increases with increasing T_{rot}, $|\tau|$, and $|T_{ex}|$. Assuming fairly moderate values of $T_{rot} = 40$ K, $\tau = -5$, and $T_{ex} = -5$ K we obtain $N_{CH_3OH} \approx 10^{16}$ cm^{-2}, which is actually a lower limit for the methanol column density. Such a high column density implies that the optical depth of the $1_0-0_0A^+$ thermal line at 48 GHz exceeds unity, and hence that the brightness temperature of this line is of the order of the gas kinetic temperature, i.e., about 40 K. The brightness temperature of the marginally detected $1_0-0_0A^+$ line (Fig. 1) is no higher than 10 K, which may be a consequence of beam dilution. As the size of the VLA beam at 48 GHz is about 1″, the source size must be no larger than 0.5″, or 3×10^{15} cm. The gas density must be no higher than a few times 10^7 cm^{-3}; otherwise, the inversion is quenched by collisions. Therefore, the H_2 column density must be of the order of 10^{22} cm^{-2}, the mass about 2×10^{-4} $M_\odot$, and the methanol abundance of the order of 10^{-6}. Similarly high abundances were found by Menten et al. [22] for Orion and by Bachiller et al. [13] for the B1 region in L1157. Accordingly, this may suggest that this object is a compact clump of post-shock gas formed by, e.g., thermal instability. However, this seems unlikely, since, in this model, it is natural to expect that the clumps producing the strongest masers are located in regions of strongest thermal emission, which does not agree with our observations. A crucial test for the compact-source model is observations at 48 GHz with higher spatial resolution: such models (like the above turbulent model) are possible only if these observations yield higher brightness temperatures in the $1_0-0_0A^+$ line towards M1 and M2 than our observations detected.

Analysis of the spectra of M1 and M2 suggests another interpretation of our results. Figure 1 shows that the M1 and M2 maser lines are double. A double thermal line with a "blue" asymmetry (i.e., with the blue component stronger than the red component) may be a signature of collapse [23]. In contrast to this, a "red" asymmetry is seen in the M1 and M2 spectra. However, we can easily show that just such an asymmetry should be observed in Class I maser lines. Strelnitskii [24] suggested that Class I methanol masers arise in collapsing protostars; our results may provide support to this idea.

Here, we present a simplified consideration of the formation of Class I maser lines in a collapsing cloud for the two most common collapse models: inside–out collapse [25], and the Larson–Penston model [26]. Our goal is to qualitatively show that a Class I line with a "red" asymmetry can be emitted

in a collapsing cloud. A detailed quantitative study of collapsing-cloud models and their applicability to the masers in L1157 requires significant observational and modeling effort, and will be developed in subsequent papers.

The model of an inside–out collapse considered by Shu [25] begins with an unstable configuration of a singular isothermal sphere. According to [25], the density and velocity in the central parts of a collapsing cloud approach $n \propto r^{-1.5}$ and $v \propto r^{-0.5}$. Points with equal radial velocities form loops (Fig. 3, upper panel). Along any given line of sight, there are two points with the same radial velocity. The difference between the brightness temperatures of the blueshifted and redshifted emission is given by

$$T_B - T_R = (T_1 - T_2)(1 - e^{-\tau_1})(1 - e^{-\tau_2}), \quad (4)$$

where τ_1 and τ_2 are the optical depths relevant to the inner and outer points, respectively. In the case of thermal emission, the line excitation temperature T_1 in the inner, denser region should be higher than T_2 in the outer, less dense region, so that $T_B > T_R$. However, in the case of inverted Class I masers, the situation is opposite. The optical depths τ_1 and τ_2 and excitation temperatures T_1 and T_2 are negative and depend strongly on the gas density: less density results in lower absolute values of the excitation temperature, at least if the density is higher than approximately 2×10^4 cm^{-3} (see Fig. 4). Therefore, in this case, $|T_2|$ should be less than $|T_1|$, resulting in a negative multiplicative factor $T_1 - T_2$. Negative τ_1 and τ_2 values provide a positive value for $(1 - e^{-\tau_1})(1 - e^{-\tau_2})$; hence, $T_B - T_R$ is negative, i.e., $T_R > T_B$, as in Fig. 1.

Note that the same "red" asymmetry should be observed when the inversion is quenched in the dense central regions (that is, T_1 and τ_1 are positive). In this case, the multiplicative factors $(T_1 - T_2)$ and $(1 - e^{-\tau_1})$ are positive and $(1 - e^{-\tau_2})$ is negative, resulting in $T_R > T_B$.

The alternative Larson–Penston model for gravitational collapse begins with a static cloud of constant density ([26] and references therein). According to the Larson–Penston model, the density distribution acquires the form $n \propto r^{-2}$ and the infall velocity is asymptotically constant and equal to 3.28 times the sound speed. The collapse velocity converges slowly to the asymptotic value, and reaches only about twice the sound speed in initial stages [26]. A schematic diagram of such a collapsing cloud is shown in Fig. 3 (lower panel). Blue-shifted emission is seen against the cosmic microwave background, with a brightness temperature of only 2.7 K, and is partly absorbed in the thermalized core (by "thermalized core" here, we mean the inner region where the gas density is high enough to quench inversion). On the contrary, redshifted emission is seen against the thermalized core, which has a brightness temperature of the order of the cloud kinetic temperature and is not absorbed. Therefore the redshifted emission should be brighter than the blueshifted emission. Thus, both inside–out and Larson–Penston collapse can yield the "red" asymmetry of Class I maser lines, as is shown in Fig. 1.

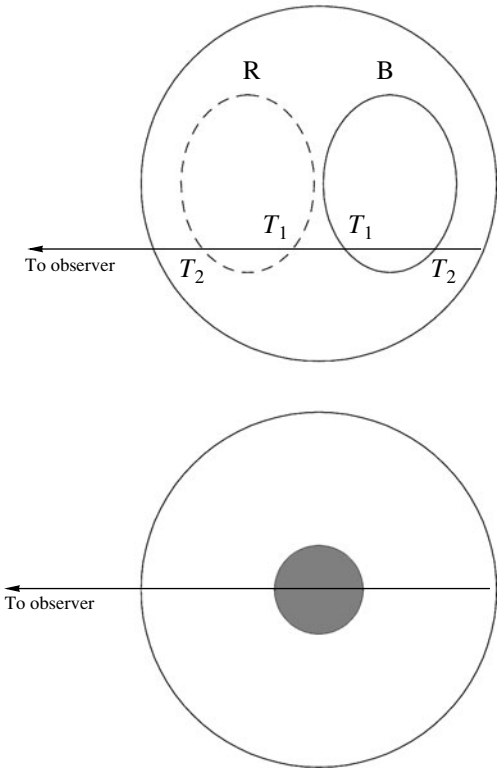

Fig. 3. Schematic of a spherical cloud in collapse. The upper panel depicts an inside–out collapse. The oval lines show regions of constant radial velocity that are redshifted (R), and blueshifted (B) relative to the systemic velocity. The lower panel depicts the Larson–Penston model. The shaded circle denotes the thermalized core.

The fact that Benedettini et al. [17] did not find a collapse signature in thermal lines of methanol and other molecules may mean that the collapse affected only the central parts of the clumps, which are smaller than their 5″ beam. In addition, the collapse signature may be blurred by the strong wings observed in most lines.

The fact that the masers arise in B0a and B1a and not in other clumps with stronger thermal methanol emission can probably be explained as follows. The collapse in B0a and B1a guarantees that the clumps are centrally condensed, which, in turn, means that the molecular column densities towards the compact central condensations are much higher than those determined by [17] with their 5″ beam. The absence

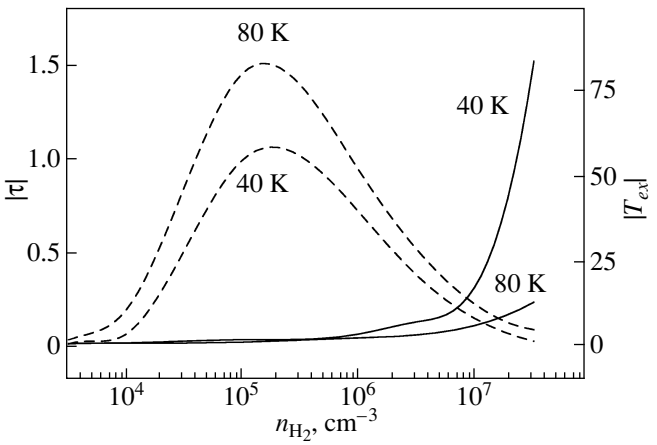

Fig. 4. Absolute values of the excitation temperature (solid curves) and optical depth (dashed curves) of the $7_0-6_1A^+$ transition as a function of gas density for 40 K and 80 K, calculated with the RADEX [27] free software using the LVG approach. The specific column density of methanol $N_{CH_3OH}/(dV/dR)$ was taken to be 10^{15} cm^{-2}/(km/s pc^{-1}) for both temperatures.

of masers in other clumps may mean that they are not so centrally condensed. In this case, the methanol column densities towards the central condensations in B0a and B1a may be higher than those in other clumps.

Thus, currently available data on methanol masers can be explained using various models. Additional observations of both methanol masers and thermal emission of related clumps are needed. In particular, the turbulence model implies the existence of weaker maser spots at 44 GHz, which may be irregularly located or form arcs or lines. Such spots could be detected using interferometric observations with higher dynamic range. On the other hand, the detection of a "collapse signature" in the spectra of other masers in regions of low-mass star formation might support the collapse hypothesis.

5. CONCLUSION

Our VLA observations of a Class I methanol maser candidate in the region of low-mass star formation L1157 have shown that the narrow line at 44 GHz is emitted by a compact, undoubtedly maser source associated with clump B0a. This clump is seen in thermal lines of methanol and some other molecules near the edge of a cavity, excavated by high-velocity gas. A much weaker compact source is associated with the clump B1a, which is brighter than B0a in thermal methanol lines. The masers may form in layers of turbulent post-shock gas. In this case, the maser emission may be beamed, so that only an observer located in or near the layer planes can observe strong masers. On the other hand, the double lines of the newly detected masers in L1157 suggest that the masers may form in collapsing clumps. A simple analysis shows that the "red" asymmetry of the detected maser lines, opposite to the "blue" asymmetry typical of thermal lines in collapsing clouds, is a natural consequence of collisional pumping of the 44 GHz transition. A detailed analysis of collapsing-cloud models and their applicability to the masers in L1157 will be given in subsequent papers.

ACKNOWLEDGMENTS

The authors are grateful to the VLA staff for the observations. This work was partially supported by the Russian Foundation for Basic Research (grant nos. 04-02-17057 and 07-02-00248) and the Basic Research Program of the Russian Academy of Sciences "Extended Sources in the Universe." P.H. acknowledges partial support from NSF grant AST-0908901. The Onsala Space Observatory is the Swedish National Facility for Radio Astronomy and is operated by Chalmers University of Technology, Göteborg, Sweden, with financial support from the Swedish Research Council and the Swedish Board for Technical Development.

REFERENCES

1. A. D. Haschick, K. M. Menten, and W. Baan, Astrophys. J. **354**, 556 (1990).
2. K. M. Menten, Astrophys. J. **380**, L75 (1991).
3. S. Kurtz, P. Hofner, and C. V. Alvarez, Astrophys. J. (Supll.) **155**, 149 (2004).
4. K. M. Menten, in *Proc. of the 3rd Haystack Observatory Meeting*, Ed. by A. D. Haschick and P. T. P. Ho, ASP Conf. Ser. **16**, 119 (1991).
5. D. M. Cragg, K. P. Johns, P. D. Godfrey, and R. D. Brown, Mon. Not. R. Astron. Soc. **259**, 203 (1992).
6. A. M. Sobolev, D. M. Cragg, and P. D. Godfrey, Astron. Astrophys. **324**, 211 (1997).

7. R. L. Plambeck and K. M. Menten, Astrophys. J. **364**, 555 (1990).
8. X. Chen, S. P. Ellingsen, and Z.-Q. Shen, Mon. Not. R. Astron. Soc. **396**, 1603 (2009).
9. S. V. Kalenskii, V. G. Promyslov, V. I. Slysh, et al., Astron. Zh. **83**, 327 (2006) [Astron. Rep. **50**, 289 (2006)].
10. S. V. Kalenskii, S. Kurtz, V. I. Slysh, et al., Mon. Not. R. Astron. Soc. Monthly Not. Roy. Astron. Soc. **405**, 613 (2010).
11. H. S. P. Müller, K. M. Menten, and H. Mäder, Astron. Astrophys. **428**, 1019 (2004).
12. L. W. Looney, J. J. Tobin, and W. Kwon, Astrophys. J. **670**, L131 (2007).
13. R. Bachiller, S. Liechti, C. M. Walmsley, and F. Colomer, Astron. Astrophys. **295**, L51 (1995).
14. F. Gueth, S. Guilloteau, and R. Bachiller, Astron. Astrophys. **307**, 891 (1996).
15. F. Gueth, S. Guilloteau, and R. Bachiller, Astron. Astrophys. **333**, 287 (1998).
16. R. Bachiller, M. Perez Gutierrez, M. S. N. Kumar, and M. Tafalla, Astron. Astrophys. **372**, 899 (2001).
17. M. Benedettini, S. Viti, C. Codella, et al., Mon. Not. R. Astron. Soc. **381**, 1127 (2007).
18. S. Liechti and C. M. Walmsley, Astron. Astrophys. **321**, 625 (1997).
19. A. M. Sobolev, B. K. Wallin, and W. D. Watson, Astrophys. J. **498**, 763 (1998).
20. V. I. Slysh, S. V. Kalenskii, I. E. Val'tts, et al., Astrophys. J. (Suppl.) **123**, 515 (1999).
21. S. V. Kalenskii, V. I. Slysh, I. E. Val'tts, et al., Astron. Zh. **78**, 31 (2001) [Astron. Rep. **45**, 26 (2001)].
22. K. M. Menten, C. M. Walmsley, C. Henkel, and T. L. Wilson, Astron. Astrophys. **198**, 253 (1988).
23. S. Zhou, in *Proc. IAU Symp. No. 178 on Molecules in Astrophysics: Probes and Processes*, Ed. by E. F. Dishoeck (Kluver, Dordrecht, 1996), p. 195.
24. V. S. Strel'nitskii, Pis'ma Astron. Zh. **7**, 223 (1981) [Sov. Astron. Lett. **7**, 124 (1981)].
25. F. H. Shu, Astrophys. J. **214**, 488 (1977).
26. R. B. Larson, Rep. Progr. Phys. **66**, 1651 (2003).
27. F. F. S. van der Tak, J. H. Black, F. L. Schöler, et al., Astron. Astrophys. **468**, 627 (2007).

Translated by S. Kalenskii